eraction Processes, 16 (1980) 227—245
Amsterdam — Printed in Belgium

A THEORETICAL ESTIMATION OF POWER REFLECTION SPECTROSCOPY AS AN ANALYTICAL TECHNIQUE

M.W. EVANS
Chemistry Department, University College of Wales, Aberystwyth, SY23 1NE, Wales.

(Received 3 October 1979)

ABSTRACT

The potential of power reflection spectroscopy is investigated theoretically in the following areas:

(i) Reflection from ionic crystals, melts and conducting media;
(ii) biomolecular suspensions;
(iii) semiconductors;
(iv) gas/solid and liquid/solid interfaces.

There are significant advantages in each area of application, especially where the angle of incidence ϕ can be varied through its $0\text{-}90^{o}$ range. Measurements near the Brewster angle are especially interesting.

INTRODUCTION

In this paper we aim to explore theoretically the potential advantages of reflection spectroscopy in several fields of application where the technique of absorption is restricted by the nature of the sample or of the experiment. For example, studies of reactions at gas-solid and gas-liquid interfaces may be carried out with advantage by reflecting a beam from the solid surface. In addition, the technique of reflection has the added advantage that both the real and imaginary parts of $\varepsilon^{*1/2}$ are measured simultaneously. Here ε^{*} is the complex permittivity.

The paper is developed as follows. Firstly we recall briefly the fundamental equations of reflection spectroscopy [1]. The next section deals with the advantages of reflecting radiation from salts, ionic and conducting media, where loss measurements require the use of very thin samples and often

blocking electrodes with associated Maxwell-Wagner losses[2]. In section 3 we apply the method to lossy material such as aqueous biomacromolecular suspensions[3] studied at low frequencies. Lastly we emphasize the use of the technique at gas/solid and gas/liquid interfaces[4].

Section 1

The measurement of power absorption coefficient on dielectric loss in absorption spectroscopy is replaced by that of the power reflection coefficient (R), which is the ratio of reflected intensity to incident intensity. If the incidence angle, ϕ, is zero, i.e. if the incident radiation is normal to the reflecting surface, then the emerging beam is unpolarized. In general, however, R has two components R_σ and R_π. If the direction of vibration of the radiation is taken with respect to the plane of incidence the component of the radiation vibrating parallel to this plane is denoted by the subscript π, and that vibrating perpendicularly by σ. The reflective power for each component is defined in terms of ϕ and the refracting angle by Fresnel's formulae:

$$\left.\begin{aligned} r_\sigma &= \sin^2(\phi-\chi)/\sin^2(\phi+\chi); \\ r_\pi &= \tan^2(\phi-\chi)/\tan^2(\phi+\chi) \end{aligned}\right] \qquad (1)$$

The angles ϕ and χ are connected by Snell's law:

$$\sin\phi = n'\sin\chi$$

where n' is the refractive index of the substance under investigation.

In general, from Maxwell's equations:

$$n^* = \varepsilon^{*\frac{1}{2}}$$

where ε^* is the complex permittivity. It follows that[1]; if $n^* = n'(1-is)$

$$R_\pi = \frac{a^2+b^2-2a\cos\phi\cos^2\phi}{a^2+b^2+2a\cos\phi+\cos^2\phi} \qquad (2)$$

$$R_\pi = R_\sigma \cdot \frac{a^2+b^2-2a\sin\phi\tan\phi+\sin^2\phi\tan^2\phi}{a^2+b^2+2a\sin\phi\tan\phi+\sin^2\phi\tan^2\phi} \qquad (3)$$

where:

$$a = \left[\tfrac{1}{2}(n^2(1-\kappa^2)-\sin^2\phi)+\tfrac{1}{2}((n^2(1-\kappa^2)-\sin^2\phi)^2+4n^4\kappa^2)^{\frac{1}{2}}\right]^{\frac{1}{2}} \qquad (4)$$

$$a^2+b^2=\tfrac{1}{2}\left[n^2(1-\kappa^2)-\sin^2\phi\right]+\tfrac{1}{2}((n^2(1-\kappa^2)-\sin^2\phi)^2+4n^4\kappa^2)^{\frac{1}{2}} \qquad (5)$$
$$+2n^4\kappa^2/\left[n^2(1-\kappa^2)-\sin^2\phi+((n^2(1-\kappa^2)-\sin^2\phi)^2+4n^4\kappa^2)\right]^{\frac{1}{2}}$$

The apparent complexity of these relations is no obstacle with available computers.

The reflection from a surface of a polarised beam of radiation is a method which is potentially more revealing than absorption spectroscopy, especially since both R_σ and R_π can be measured throughout the range of ϕ, the incident angle. At the Brewster angle, which we define by $\phi_\beta = \tan^{-1} \varepsilon_\infty^{1/2}$, where ε_∞ is the high frequency limit of the real part of ε^*, some interesting effects are revealed by the theoretical models we develop in the following sections. If these were investigated experimentally, a new source of spectral information would be utilised.

Section 2

Reflection from Salts and Conducting Media

For an isotropic crystal, the dielectric permittivity is [5]

$$\varepsilon^* = 1+4\pi\chi_{elec} + \chi_{ion}$$

where χ_{elec} is the susceptibility due to the distortion of the electron distribution by the electromagnetic field and χ_{ion} arises from ionic displacements during lattice vibrations. It is usual to define a high frequency or 'optical' dielectric constant by the relation:

$$\varepsilon_\infty = 1 +4\pi\chi_{elec} \qquad (6)$$

o develop theoretical expressions for the reflection spectrum from an ionic attice we may follow the classical Born analysis[5] of an isotropic (cubic) onic, lossy lattice, with the equation of motion:

$$\ddot{w} + 2\pi\gamma\dot{w} + 4\pi^2\nu_o^2 w = \frac{eE_o}{\mu} e^{-2\pi i\nu t} \qquad (7)$$

ere μ is a reduced mass, defined by:

$$\frac{1}{\mu} = \frac{1}{M_1} + \frac{1}{M_2}$$

here M_1 is the mass of ion type 1 and M_2 that of type 2. w is a relative isplacement of the ionic coordinates, γ is a damping factor to allow for he loss process, and ν_o is the frequency of the optical lattice mode. t follows that:

$$\varepsilon'(\nu) = \frac{e^2(\nu_o^2 - \nu^2)}{\pi\mu V_c\left[(\nu_o^2-\nu^2)^2+\nu^2\gamma^2\right]} + \varepsilon'_\infty \qquad (8)$$

$$\varepsilon''(\nu) = \frac{\nu\gamma e^2}{\pi\mu V_c\left[(\nu_o^2 - \nu^2)^2+\nu^2\gamma^2\right]} \qquad (9)$$

here V_c is the volume of the unit cell. If the primitive cell contains more than one infra-red active frequency eqns (8) and (9) can be generalised y summing over such frequencies. The ionic charges, e, are replaced by an ffective charge:

$\sqrt{\mu}\left(\frac{\partial m}{\partial Q_k}\right)$, where $\left(\frac{\partial m}{\partial Q_k}\right)$ is the equilibrium value f the derivative of the dipole momemnt with respect to the mass-weighted ormal coordinate Q_k - In general, therefore, eqns (8) and (9) take the orm:

$$\varepsilon' = \frac{1}{\pi V_c} \sum_k \left(\frac{\partial m}{\partial Q_k}\right)^2 \left(\frac{\nu_{o,k}^2 - \nu^2}{(\nu_{o,k}^2-\nu^2)^2 + \nu^2\gamma_k^2}\right) + \varepsilon'_\infty \qquad (10)$$

$$\varepsilon'' = \frac{1}{\pi V_c} \sum_k \left(\frac{\partial m}{\partial Q_k}\right)^2 \frac{\nu\gamma_k}{(\nu_{o,k}^2 - \nu^2)^2 + \nu^2\gamma_k^2} \qquad (11)$$

To illustrate the use of eqns (1) to (11) we take some recent data from a paper by Hiraishi, Taniguchi, and Takahashi[6] on radiation reflected from the surface of lithium potassium sulphate single crystals at infra-red frequencies, and concentrate particularly on the R_π component near the Brewster angle:

$$\phi_\beta = \tan^{-1}\left|1+4\pi\chi'_{elec}\right|^{\frac{1}{2}} \qquad (12)$$

The experimental reflection data from about 50 cm^{-1} to 2000 cm^{-1} can be reproduced almost perfectly by eqns (10) and (11) for an incidence angle of $\phi = 20^0$ in R_σ polarisation for both E_1 and A symmetry species present in the crystal. The theoretical spectra for the A species are reproduced in fig (1). However, using now the value of $\varepsilon_\infty = 2$ listed by these authors we may investigate theoretically the effect of varying the incidence angle ϕ on the bandshapes and band intensities. Comparison with the actual experimental data then provides us with a means of investigating the point of breakdown of the bandshape model used. In R_σ polarisation near the Brewster angle the bandshapes and intensities are changed significantly, but dramatically so in R_π polarisation (fig. 1(a)) where the attenuation is heavy, of course, but not complete. A powerful, polarised, incident, tunable laser beam reflected at the Brewster angle in R_π polarisation could be detected to build up the type of information illustrated theoretically in fig. 1(b). Note that new peaks and troughs appear in the spectrum near ϕ_β as a result of the fundamental equations of reflectivity which are derived from Maxwell's equations in the relevant context. Also, at very high frequencies the R_π attenuation increases steadily to a peak (fig.1(c)) which could be used for the purposes of characterisation provided the attenuation problems could be met.

Next we investigate the possibility of characterising the dielectric relaxation processes of electrolyte solutions[7] using reflection of radiation

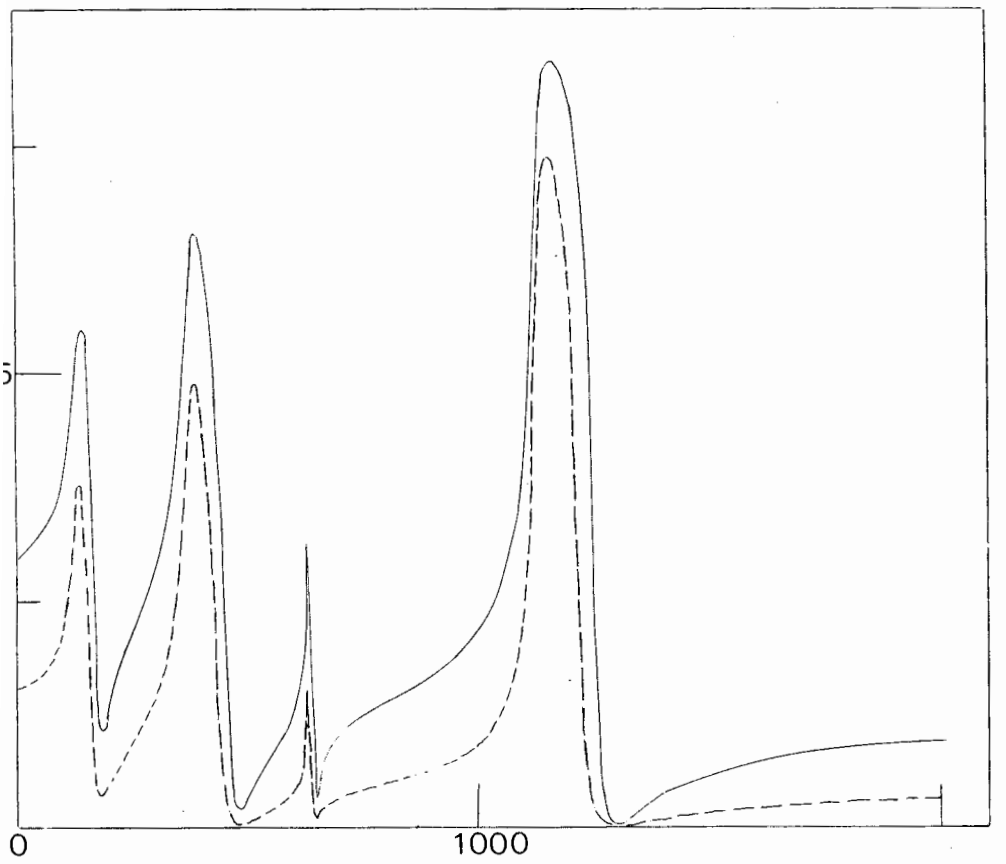

Fig.1(a)

Figure (1)

(a) Calculated reflection spectra for lithium potassium sulphate in polarisation, using eqns. (10) and (11) with the parameters of Hiraishi et al[6].

- - - - $\phi = 20^0$

———— $\phi = \tan^{-1} \varepsilon_{\infty}^{1/2}$; $\varepsilon_{\infty} = 2.0$, the Brewster angle.

Ordinate: R_0 ; abscissa $\bar{\nu}/cm^{-1}$

(b) The same in π polarisation.

Ordinate: $-\log_e R_0$; abscissa: $\bar{\nu}/cm^{-1}$

(c) High frequency part of fig (1.b)

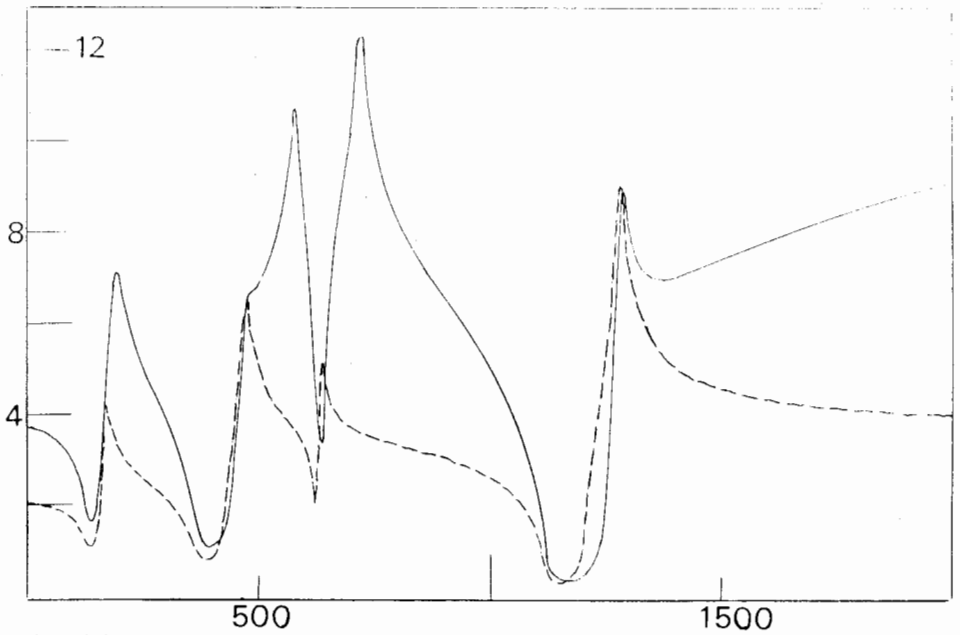

Fig.1(b)

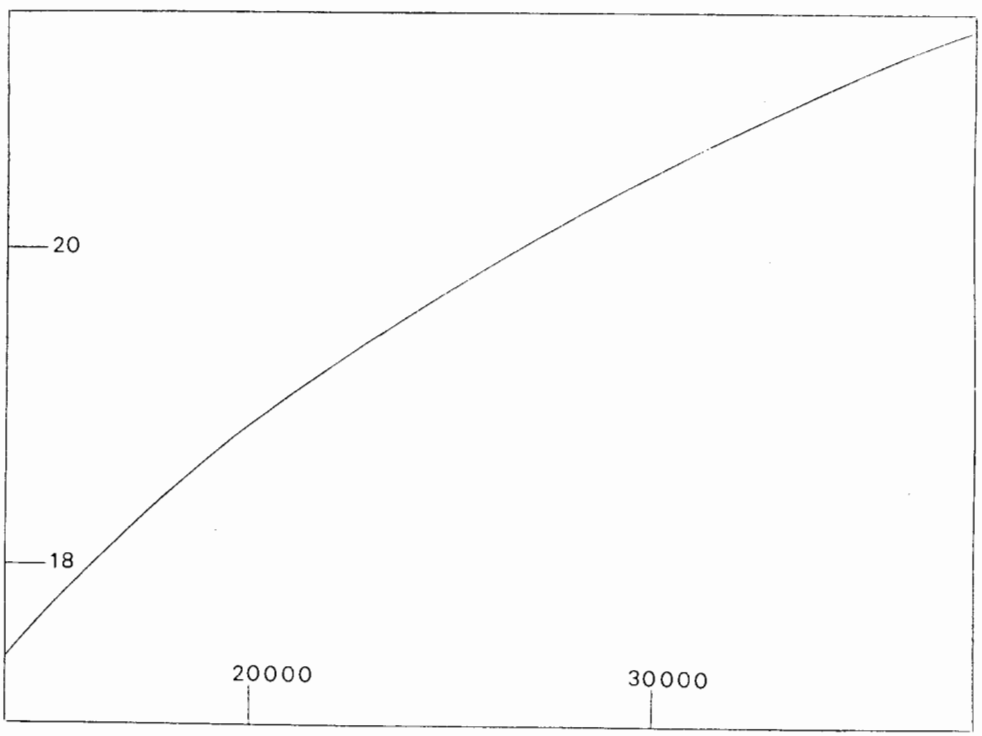

Fig.1(c)

over a broad sweep of frequencies. In these media the complex permittivity is expressed in the corrected form:

$$\varepsilon^* = \varepsilon' - i(\varepsilon'' - \sigma/\omega\varepsilon) \qquad (13)$$

where σ is the conductivity, a real quantity. The Debye/Falkenhagen effect, however, produces a complex conductivity so that, strictly, ε' should also be corrected for the effect. Moreover the form of eqn. (13) already implicitly assumes that the microscopic behaviour of the solution allows this kind of separation of terms. This is by no means clear, but for our present purposes we take eqn. (13) as an useful empiricism. In eqn. (13) ε is the absolute permittivity of free space.

In investigating conducting solutions dielectrically there is the problem of measuring a complex permittivity characterised by a very high loss tangent when working with the low frequency end of the spectrum (e.g. below 100 MHz). On top of this it is not possible to obtain the response of bulk liquid without involving simultaneously that of the solution-electrode interface. Below 100 MHz the conventional methods involve bridges of the Schering type, for example, ε' being proportional to the cell capacitance, $''_{\omega}$ to the cell conductance, after due correction for transmission line effects, edge effects, and electrode polarisation. The relevant corrections are then often complicated and difficult to apply. Recently, however, there has been a renewed interest in these systems because of their importance in areas of biological activity. Above about 100 MHz the accuracy in ε' may be poor from conventional methods because it is calculated often as the difference between two large numbers. Measurements on fused salts such as sodium nitrate are particularly prone to this drawback. Finally, time-domain and sweep-frequency methods have not improved matters significantly.

The very simple technique of reflecting a beam of radiation from such fused solid or conducting liquid surfaces may be of use in supplementing

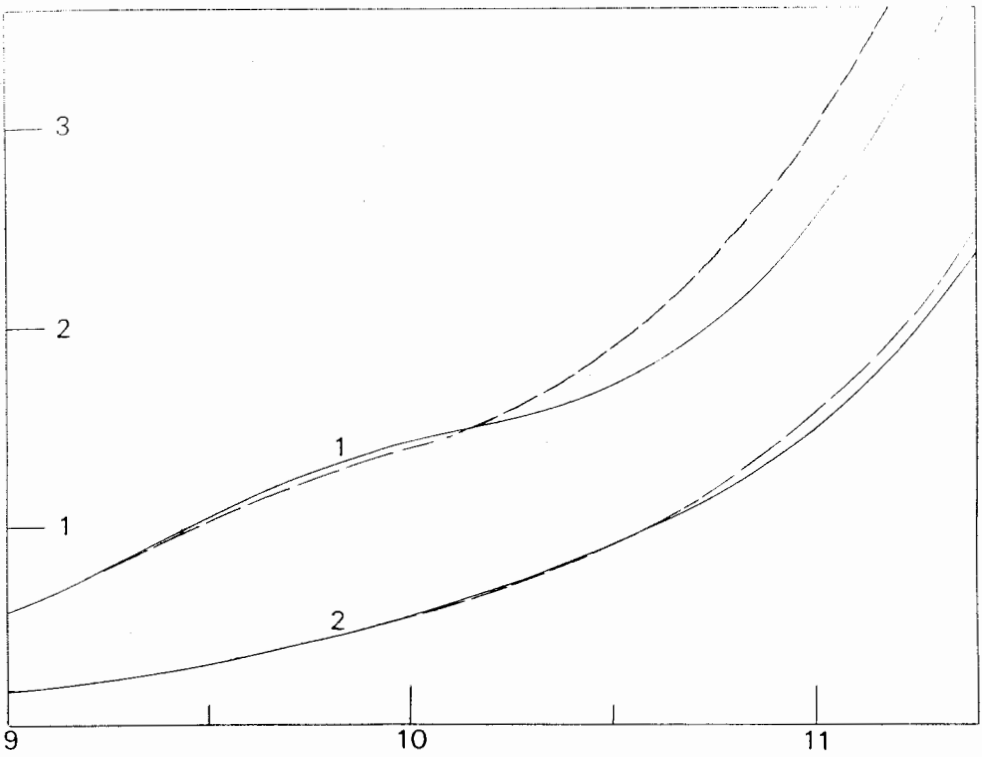

Figure (2)

Low frequency reflectivity in conducting media in R_{π} polarisation at the Brester angle.

——— Three variable Mori model of the orientational autocorrelation function.

- - - Internal field correction to the Mori model as used by Lobo et al.

(1) $\sigma = 10^{-2}\ \Omega^{-1}\ cm^{-1}$;

(2) $\sigma = 10^{-1}\ \Omega^{-1}\ cm^{-1}$

Ordinate: $-\log_e R_{\pi}$; Abscissa: $\log(\omega)$

the conventional methods when these prove of uncertifiable accuracy. In principle, the more conducting the medium, the easier it becomes to detect the reflected radiation. Fig. (2) is a theoretical estimate of the R_{π} component at the Brewster angle using two models[7-10] of the molecular motion, with and without an internal field correction. One is a Mori three variable approximant applied directly to the orientational autocorrelation function[8], the internal field being accounted for by the method of Lobo, Robinson and Rodriquez[11], who used dielectric friction as envisaged by Scaife[12] and by Nee and Zwanzig[13]. Fig. (1) shows that even at the heavily attenuating Brewster angle of incidence, the lower the frequency and the higher the conductivity the easier it becomes to measure the reflectivity R_{π} (or R_{σ}) and thereby the complex permittivity ϵ^{*}. Real and imaginary parts are, of course, measured simultaneously. At frequencies lower than about 100 MHz the experimental difficulties are as follows:

(i) Control of polarisation;

(ii) Control of beam direction;

(iii) Detection.

At 100 MHz and into the microwave region conventional waveguide techniques could be adapted straightforwardly. The necessary apparatus for work at far infra-red frequencies (THz) is already available, designed by Birch[14]. Typical theoretical reflection spectra in this region are illustrated in figs (3) and (4), the variation of incident angle, Ø, proving particularly useful when characterising liquid state molecular dynamics with theoretical models.

Section 3

Reflection Spectroscopy of Biological Systems

The difficulties of making conventionally dielectric measurements[3] on biological systems have been known for many years. These are usually carried out on aqueous media, and static permittivities can reach into the

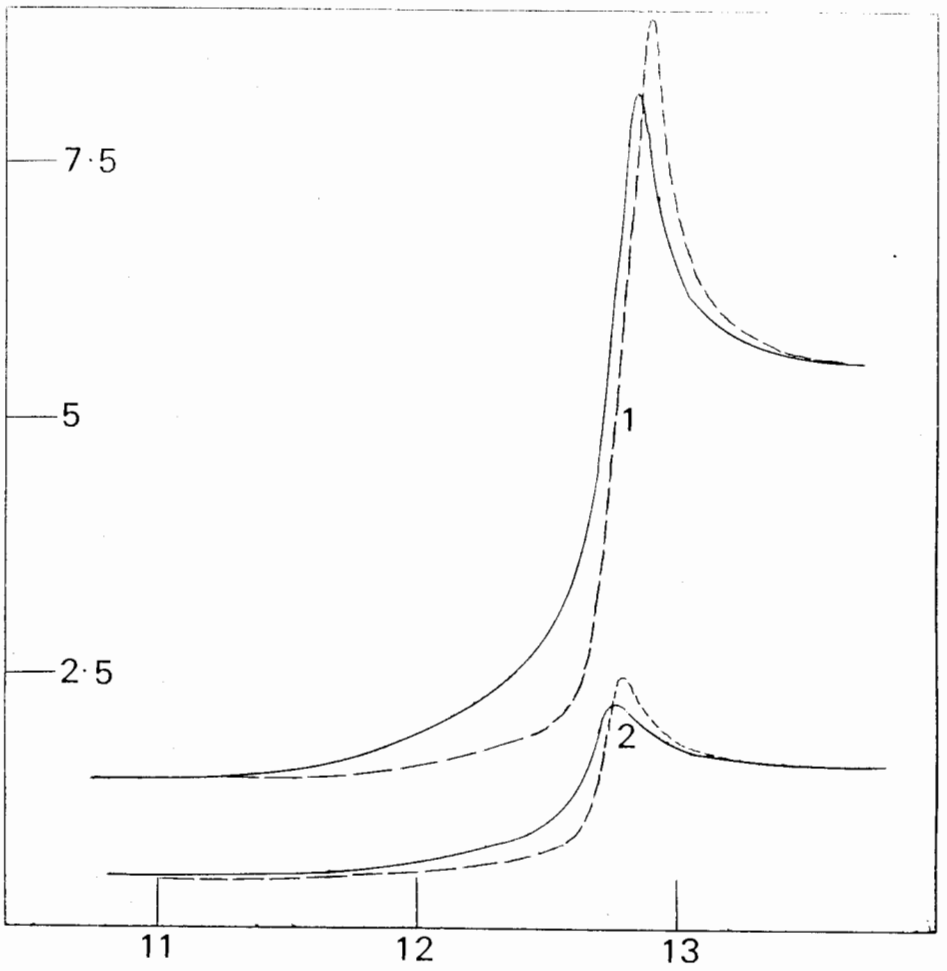

Figure (3)

Reflectivity spectra: (1) R_{π} ; (2) R_{σ} for a dipolar liquid.

---- Mori three variable theory

—— Mori theory corrected for the internal field using the Method of Lobo et al. $\phi = 50^{0}$.

Ordinate: $-\log_{e} R$; Abscissa: $\log(\omega)$

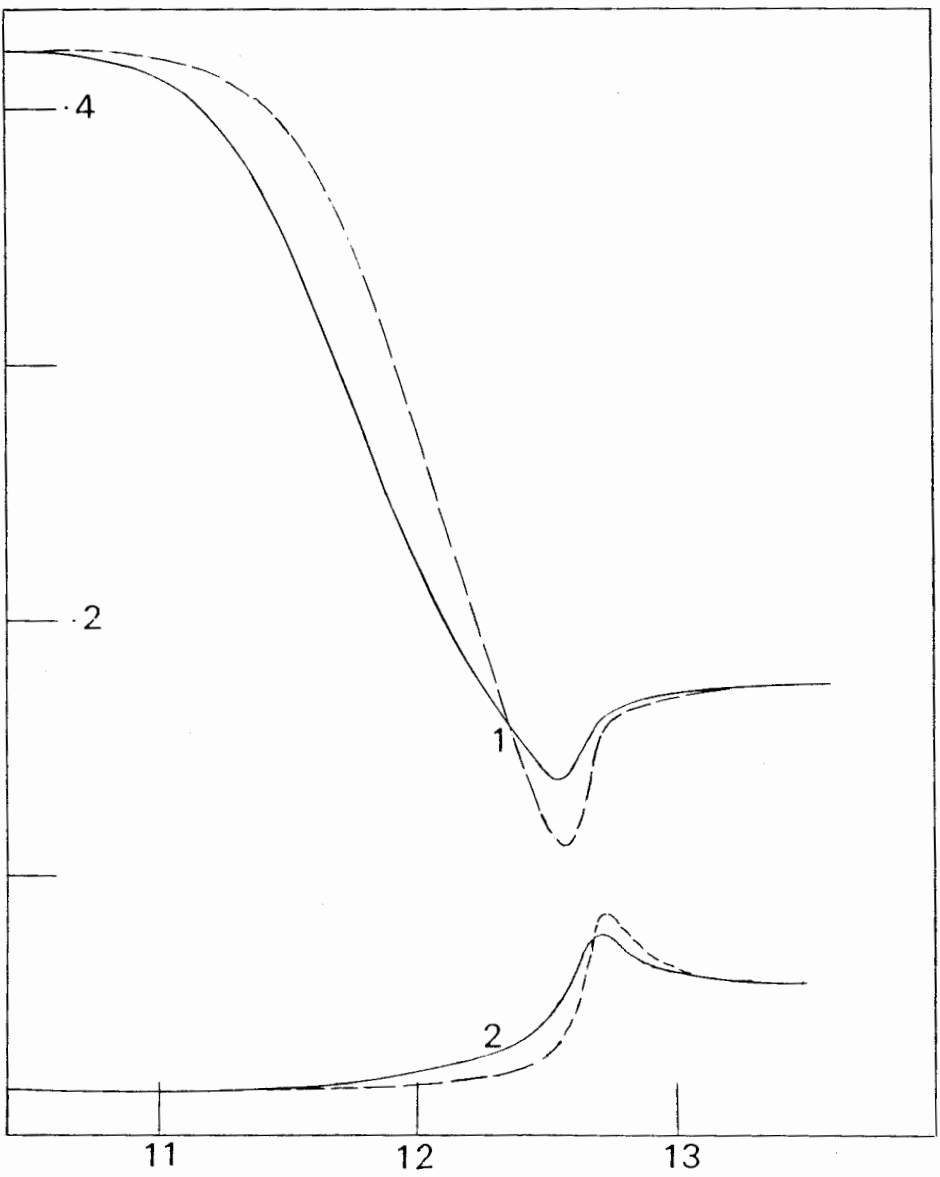

Figure 4

10^6 order of magnitude. Maxwell/Wagner, or interfacial, effects are an added complication because of the size of the molecules under investigation. Enormously large dielectric increments can be obtained through effects due to polarization of counterion distribution in the interface between the particle and the surrounding fluid medium. This gives rise to intense absorption at low frequencies (the α process, for example, in the range 1 - 10 kHz). These properties are changed remarkably by the application of an external field, which is, of course, the measuring field in conventional terms. However, if reflectivity methods could be applied in the kHz range (radio frequencies) the applied electric field could be increased in strength to the point of breakdown, or pulsed past this point, the dielectric properties being monitored through the reflection coefficient $R = \frac{1}{2}(R_\sigma + R_\pi)$. The reflectivity measurements of the surface of the biological system would usefully complement conventional measurements of the bulk using bridge and capacitors. In fig (5) we illustrate a hypothetical (model) reflectivity curve for a dielectric increment of $\varepsilon_o = 1000$, $\varepsilon_\infty = 3$, ϕ = one radian. The R_π and R_o curves are corrected again for internal field effects as in fig. (2). The reflected intensity is sufficient to be measurable provided the incoming and reflected beams can be controlled and detected experimentally. Clearly the higher the dielectric increment the easier it is to reflect a beam from the surface of the material under consideration. This is used to advantage in the next section, where we consider semiconductors and gas/solid interfaces.

Section 4

Semiconductors and Gas-Solid Interfaces

The far infra-red absorptions of a semiconductor are naturally very intense but provide useful information on a variety of phenomena[15]. These include plasma absorption at low frequencies and absorption by transverse optical lattice modes at higher frequencies, reviewed by Chantry. There

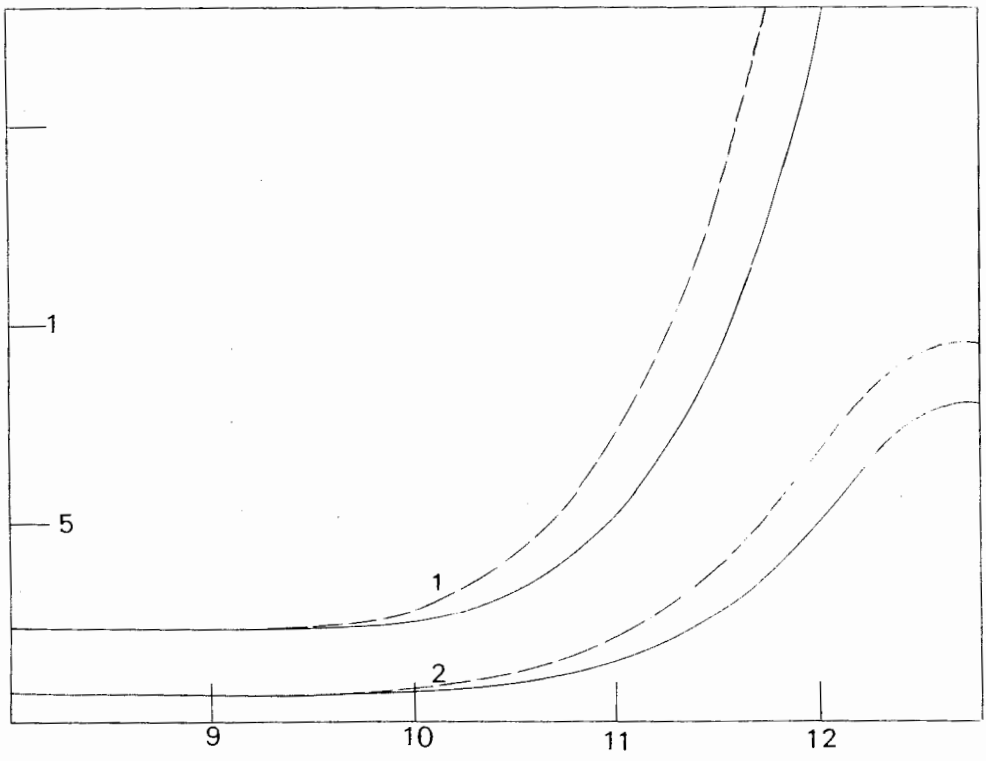

Figure 5

Low frequency reflectivity for an intensely absorbing species.

(1) $R_{\parallel}$; (2) R_{θ} ; —— 3 variable Mori theory and --- Lobo theory.

ε_{∞} = 1000, ω_{p} = 3; $\emptyset$ = 1 radian.

Ordinate - $\log_e R$; Abscissa : - $\log(\omega)$.

will be absorption due to cyclotron resonance if the specimen is in a magnetic field. There are also detectable features due to localized phonons at impurity lattice sites, or due to the breakdown of the usual selection rules caused by other phenomena such as unharmonicity. However, the spectrum is interpretable in terms of important parameters, such as N_e, the number of electrons per cm^3, ω_p the electron - ion collision

frequency, and m^* the effective mass of the particle of charge q under investigation. For example, when employing the technique of far infra-red cyclotron resonance spectroscopy the particle m* will rotate in a circle with a cyclotron frequency $\omega_c = qH/2\pi m^*c$, where H is the applied magnetic field strength. In semiconductors, the resonance can arise both from the electrons and the holes, and for both m* can differ greatly from m. As in plasmas, where electron - ion collisions have the effect of making the plasma absorptive and to keep the refractive index real, we have for the real and imaginary parts of ε^*:

$$\varepsilon' = \varepsilon_L [1 - \nu_p^2 / (\nu^2 + \nu_e^2)] \tag{14}$$

$$\varepsilon'' = \varepsilon_L \nu_p^2 \nu_e / [\nu(\nu^2+\nu_e^2)] \tag{15}$$

Here ν_p is the plasma frequency, given by:

$$\nu_p^2 = (N_e e^2/\pi m^* \varepsilon_L) \tag{16}$$

and ε_L is the lattice dielectric constant. As $\nu \to \infty$ we have $\varepsilon' \to \varepsilon_L$. The Brewster angle is therefore $\tan^{-1} \varepsilon_L^{1/2}$. Birch has designed an apparatus for reflectivity measurements in the far infra-red of semiconductors at normal incidence (ϕ = o). From the measured reflection spectrum and its measured minimum, the plasma frequency can be calculated, and N_e calculated for a given m*.

It is clear that reflectivites at both polarisations over a range of ϕ will be a source of extra information, especially when considering bandshape theories more complicated than eqns (14) and (15). Some reflectivity curves from eqns (14) to (16) are illustrated in fig (6). Again, near the Brester angle, the spectrum is significantly different in the R_η polarisation and is therefore a useful source of information on bandshape behaviour.

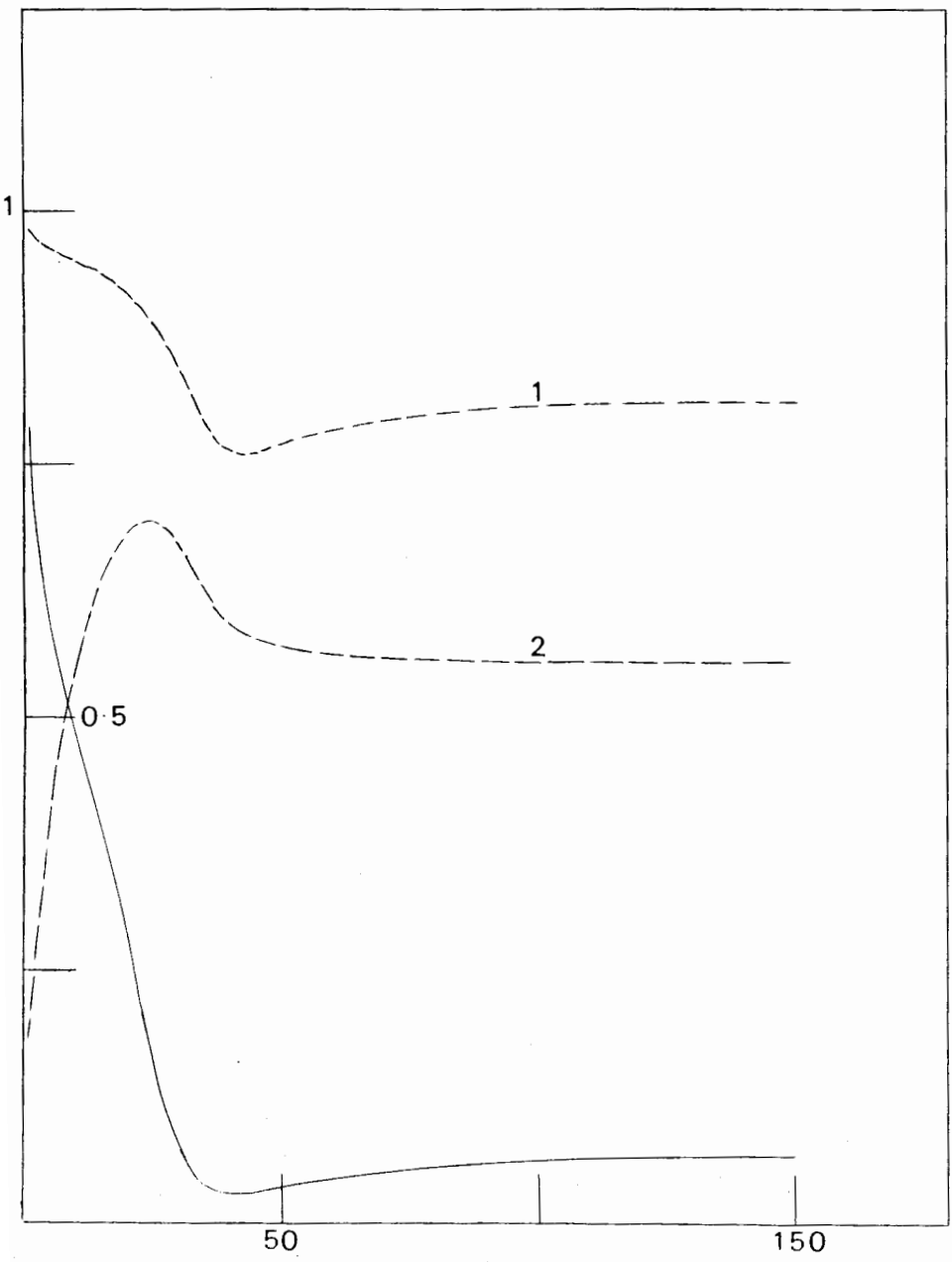

Figure 6

Reflectivity spectra from eqns (14) and (15) for various angles ϕ;

(1) $R_{\parallel}$; (2) $R_{\perp}$.

Ordinate - $\log_e R$; Abscissa: $\log (\quad)$.

Finally in this paper we consider qualitatively some possibilities of applying reflection spectroscopy to the study of gas-solid interactions. Recently Adelman and co-workers [4] have developed a theory of the many-body chemical dynamics pertinent to this problem by adopting a continued fraction formalism similar to that of Mori [16]. The formal Mori framework is of wide applicability in that it reduces the general multi-body problem to one of determining experimentally a vastly smaller number of equilibrium thermodynamic time averages.

In the simplest case the equation of motion governing the system is a generalised Langevin equation:

$$\ddot{\underline{R}}(t) = -\frac{\partial W}{\partial \underline{R}} \quad (\underline{r}, R); \tag{17}$$

$$\ddot{\underline{r}}(t) = -m^{-1}\frac{\partial W}{\partial \underline{r}} \quad (\underline{r}, R) - \omega_e^2\,\underline{r}\,(t) + \int_0^t \theta\,(t-\tau)\underline{r}(\tau)d\tau + \underline{f}\,(t) \tag{18}$$

where $\underline{R}$ and M and $\underline{r}$ and m are respectively the coordinates and masses of the incident gas atom and struck surface atom; $W(\underline{r}, \underline{R})$ is the atom-solved potential energy function. Eqn (17) is the gas atom equation of motion and the heatbath response function $\theta(t)$ is that in the absence of the gas atom. This is rigorous only if the solid is perfectly haromonic, but is otherwise an approximation. The potential energy function $W(\underline{r}, \underline{R})$ can include the static influence of the heatbath solid atoms; i.e. it can depend on the equilibrium position of all atoms in the solid. The damping kernel $\theta(t)$ contains the following effects:

(i) The influence of the nuclear motion of all heatbath solid atoms on the dynamics of the primary system

(ii) Any influence of non-nuclear degrees of freedom, such as electronic or spin, on atomic motion.

(iii) Anharmonicities in the primary system motion.

The influence of gas-solid reactions on an infra-red spectrum such as that of fig (1) could be detected by reflection spectroscopy provided

$\underline{r}(t)$ of eqn. (13) were replaced by such as the relative ionic displacement of eqn. (7), so that the correlation function $\langle \underline{r}(t).\underline{r}(o) \rangle$ could be transformed into an observable infra-red reflection spectrum, using an approximant of the continued fraction expansion of eqn. (18). The measurement of laser radiation reflected from the reacting surface would be relatively straightforward.

Discussion

In this paper we have briefly considered the advantages of using reflection spectroscopy to investigate the dielectric properties of media which present problems when using conventional absorption or bridge techniques. These problems consist of intense absorption, electrode interface effects, Maxwell-Wagner loss, bridge instabilities, etc. which could be remedied using the 'non-contact' technique of reflection spectroscopy. The latter is especially interesting in R_{π} polarisation near the Brewster angle of incidence provided the problems of attenuation would be overcome. In heavily absorbing media such as aquous biomolecular suspensions the low frequency measurement of reflectivity, if experimentally feasible, could usefully complement the conventional bridge techniques. At far infra-red frequencies, on the other hand reflection measurements of semiconductors are already possible, which in principle provide useful information on charge carrier density and behaviour near the plasma edge. Extension of theoretical techniques to bandshape analysis in semiconductors would benefit from measurements using a variety of incident angles $\emptyset$.

Acknowledgements

S.R.C. is acknowledged for financial support, and Dr. G. J. Davis for motivating this work.

References

1. W. Brugel, An Introduction to Infra-red Spectroscopy, Methuen, London, 1962.

2. J.-C. Lestrade, J.-P. Badiali and H. Cachet, in 'Dielectric and Related Molecular Processes', Vol. 2, p.106, Chem. Soc. Specialist Per. Report, London (1975).

3. G. Schwartz, ref. (2), Vol. 1 (1972).

4. S.A. Adelman, Adv. Chem. Phys., preprint.

5. G. Turrell, Infrared and Raman Spectra of Crystals, Academic Press, London and New York, 1972.

6. J. Hiraishi, N. Taniguchi and H. Takahashi, J. Chem. Phys., 65 (1976) 3821.

7. M. W. Evans, G. J. Evans, and A. R. Davies, Adv. Chem. Phys., in press.

8. G. J. Evans and M. W. Evans, J. Chem. Soc., Faraday Trans. II, 72 (1976) 1169.

9. M. W. Evans, Adv. Mol. Rel. Int. Proc., 10 (1977) 203 - 271.

10. G. J. Evans and M. W. Evans, ibid., 9 (1976) 87.

11. R. Lobo, J. E. Robinson and R. Rodriguez, J. Chem. Phys., 59 (1973) 5992.

12. B. K. P. Scaife, ed., Complex Permittivity, English Univ. Press, London, (1971).

13. T. W. Nee and R. Zwanzig, J. Chem. Phys., 52 (1970) 6353.

14. J. Birch, communication, N.P.L. internal report.

15. G. W. Chantry, Submillimetre Spectroscopy, Academic, (1971).

16. H. Mori, Prog. Theoretical Phys., 33 (1965) 423.